Energy 139 (2017) 935–946

Contents lists available at ScienceDirect

Energy

journal homepage: www.elsevier.com/locate/energy

Sequencing the features to minimise the non-cutting energy consumption in machining considering the change of spindle rotation speed

Luoke Hu [a], Ying Liu [b, *], Niels Lohse [b], Renzhong Tang [a], Jingxiang Lv [c], Chen Peng [a], Steve Evans [d]

[a] Key Laboratory of Advanced Manufacturing Technology of Zhejiang Province, College of Mechanical Engineering, Zhejiang University, Hangzhou 310027, China
[b] School of Engineering, University of Glasgow, University Ave, Glasgow G12 8QQ, United Kingdom
[c] Key Laboratory of Contemporary Design and Integrated Manufacturing Technology, Ministry of Education, Northwestern Polytechnical University, Xi'an 710072, China
[d] Institute for Manufacturing, Department of Engineering, University of Cambridge, Cambridge CB3 0FS, United Kingdom

ARTICLE INFO

Article history:
Received 14 November 2016
Received in revised form
21 July 2017
Accepted 8 August 2017
Available online 13 August 2017

Keywords:
Non-cutting energy consumption
Sustainable manufacturing
Spindle rotation
Feature sequencing
Ant colony optimisation

ABSTRACT

A considerable amount of energy consumed by machine tools is attributable to non-cutting operations, including tool path, tool change, and change of spindle rotation speed. The non-cutting energy consumption of the machine tool (NCE) is affected by the processing sequence of the features of a specific part (PFS) because the plans of non-cutting operations will vary based on the different PFS. This article aims to understand the NCE between processing a specific feature and its pre- or post-feature, especially the energy consumed during the speed change of the spindle rotation. Based on the developed model, a single objective optimisation problem is introduced that minimises the NCE. Then, Ant Colony Optimisation (ACO) is employed to search for the optimal PFS. A case study is developed to validate the effectiveness of the proposed approach. Two parts with 12 and 15 features are processed on a machining centre. The simulation experiment results show that the optimal or near-optimal PFS can be found. Consequently, 8.70% and 30.42% reductions in NCE are achieved for part A and part B, respectively. Further, the performance of ACO for our specific optimisation problem is discussed and validated based on comparisons with other algorithms.

1. Introduction

According to the International Energy Agency, nearly 1/3 of the global energy consumption and 36% of carbon dioxide emissions are attributable to manufacturing industries [1], and the electricity consumption of machine tools accounts for more than half of the total U.S manufacturing electricity consumption [2]. Thus, reducing the energy consumption of machine tools during the use phase is a significant topic for both academic research [3] and industrial application [4]. The energy consumption of machine tools can be reduced by replacing the existing traditional machines with the advanced energy-efficient machines that have the energy-recycling devices [5] and the efficient power generation [6] and distribution [7] systems, but it greatly increases the financial burden on the enterprises and it is not economically sound for the enterprises to abandon the existing machines [8]. Considering economic efficiency, our research aims to reduce the energy consumption of the existing machine tools without purchasing additional energy-saving devices.

The machining energy consumption of a machine tool (MTE) accounts for a majority of its total energy consumption [2]. The MTE is defined as the energy consumed by the machine tool for completing a feasible processing plan for a specific part, which can be divided to two types: non-cutting energy consumption and cutting energy consumption of the machine tool (NCE and CE) [9]. The NCE is defined as the energy consumed for the non-cutting operations of the machine tool, including tool path, tool change, and change of spindle rotation speed [10]. Generally, the NCE

* Corresponding author.
E-mail address: Ying.Liu@glasgow.ac.uk (Y. Liu).

http://dx.doi.org/10.1016/j.energy.2017.08.032

accounts for more than 30% of the MTE [10]. The CE is defined as the energy consumed when a part is actually cut by a machine tool. It has been proved that the value of the CE is affected by the processing sequence of the features of a part (PFS) [11]. Thus, finding the PFS which results in a smaller value of CE has been confirmed to be an effective energy consumption reduction approach [12]. However, the potentiality for this approach to reduce the NCE has not been well explored. Hu et al. [13] considered both the NCE and the CE while adjusting the PFS to reduce the MTE, but the detailed model for the NCE has not been provided. Besides, the CE model is redundant for the part without volumetric interaction among the features, but it has not been identified and removed from the existing MTE model.

For the NCE, the modelling work for the energy consumption of the machine tool during tool path (TPE) and tool change (TCE) has been developed by Hu et al. [14]. The TPE is defined as the energy consumed by the machine tool for moving the cutter to the right position to begin the actual cutting and the TCE is defined as the energy consumed by the machine tool for changing and selecting the right cutter [14]. However, the energy consumption of a machine tool during the change of spindle rotation speed (SCE) has been ignored. The SCE is defined as the energy consumed by the machine tool when the spindle rotates from a low (high) speed to a high (low) speed [15]. The SCE accounts for nearly 14% of the total NCE [10] and has energy-saving potentials [15]. The SCE can be subdivided into energy consumptions of the machine tool for the spindle acceleration (ASE) and deceleration (DSE). The PFS can affect the value of the SCE within the NCE, because the difference between the spindle rotation speeds of a pair of features on the PFS can vary if any of the features is replaced by another feature. Based on this discovery, the main novelty of this paper is to reduce the NCE with the SCE included through feature sequencing, and the proposed model and optimisation approach are the main contributions. The SCE can be directly obtained by the experiment measurements according to the start and end speeds. When using this method, the experiment measurements must be conducted again once the value of the start or end speed is changed, and it is laborious. To reduce the experiment costs, it is an innovation of this paper to introduce an empirical model to predict the SCE. It should be noted that the experiment is also required to develop the empirical model, but after obtaining the model, the SCE between any two spindle rotation speeds can be predicted without further experiments. In the optimisation work, Hu et al. [13] has verified that Genetic Algorithm (GA) can effectively solve the energy-aware feature sequencing problem when the MTE is regarded as the optimisation objective. When the optimisation objective is changed to the NCE which considers the SCE, the performance of GA may become inferior. A purpose of the optimisation work delivered in this paper is to present and validate an effective algorithm for solving the new single objective optimisation problem.

Based on the above, this study aims at understanding the SCE and integrating the developed SCE model with the existing NCE model which only considered the TPE and the TCE. Then, a model to depict the NCE between processing a specific feature and its pre- or post-feature has been further developed. The single objective optimisation in this research is to minimise the NCE through finding the optimal PFS. According to preliminary studies, Ant Colony Optimisation (ACO) is employed and modified as the optimisation approach to search for the optimal PFS for its good performance in solution quality [16] and computation speed [17]. Based on the case study, the proposed approach is demonstrated and its performance is compared and validated. In this study, it is assumed that all of the required processing for a part can be finished on a single machine tool.

The remainder of the paper is organised as follows. The background and motivation are given in the next section. The problem description and the model for the NCE are presented in Section 3. In Section 4, the working procedures of ACO for solving the aforementioned optimisation problem are described. Case studies are conducted to demonstrate and discuss the developed approach in Section 5, and a brief summary and future work are given in Section 6.

2. Background and motivation

The reduction of NCE has been the topic in the previous energy-aware feature sequencing studies. For example, a mathematic model was developed to reduce the NCE, including the TPE and the TCE by adjusting the PFS [14]. However, the model ignored the SCE resulting from the difference between the spindle rotation speeds of a pair of features on the PFS. The SCE accounts for nearly 14% of the total NCE [10], and it has energy-saving potentials [15]. In related studies considering the SCE, a mathematic model was developed where the value of the SCE was assumed as a constant [18]. In addition, a feature precedence graph was generated to identify the manufacturing precedence constraints, and the value of the SCE was also assumed as a constant [19]. A main limitation of these models is that they use an inaccurate and oversimplified SCE model. For example, the value of the SCE between all pairs of features in a part has not been set to a variable that considers the actual values resulting from the required acceleration or deceleration. In fact, the SCE is dependent on the start and end speeds of the spindle rotation between the features. Moreover, the data for the SCE were made up, which weakens the accuracy of the model and skews the results.

The value of the SCE can be accurately obtained by the experiment measurements according to the start and end speeds [15]. When using this method, the experiment measurement must be conducted again once the value of the start or end speed is changed. To reduce the experiment costs, it is important to develop a SCE model to predict the value of the SCE according to the difference between two spindle rotation speeds. To obtain the SCE model, Shi et al. [20] developed a quadratic model to predict the energy consumption of a machine tool for the acceleration of the spindle rotation (ASE) from measured power data. However, the start speed of the spindle rotation can only be set to 0 rpm. To predict the ASE from an arbitrary low speed to a higher speed, a model based on the spindle torque was proposed [21]. The coefficients in the model were obtained by the experiments, and the prediction accuracy achieved 90% [21]. However, the model is unable to predict the energy consumption of a machine tool for the deceleration of the spindle rotation (DSE). A model for the DSE was developed by multiplying the torque with the angular velocity [22], but the parameters used in this model, such as friction torque, are difficult to acquire for a specific machine tool. The results of these previous studies do not yet provide a comprehensive SCE model but can be used as precursor to develop our model for predicting the SCE between processing a specific feature and its pre- or post-feature.

After developing the mathematic model, the algorithms can be employed to search for the optimal PFS which results in the minimisation of the NCE with the SCE included. Hu et al. [13] has proved that Genetic Algorithm (GA) can effectively solve the energy-aware feature sequencing problem when the MTE is regarded as the optimisation objective. When the optimisation objective is changed to the NCE, the performance of GA may become inferior. So far, the specific algorithms to minimise the NCE have received little attention. For the related time-aware feature sequencing problem, plenty of algorithms, such as deterministic algorithms and meta-heuristics, have been employed in the literature. These works can be used as references for the algorithms selection to minimise our

objective. Traditionally, the deterministic algorithms, such as dynamic programming [23] and branch-and-bound method [24], have been used to find the global optimal PFS which results in the minimisation of machining time [23]. However, they are only suitable for solving the small-to-medium sized problems because the computation time sharply increases when the target part has more than 20 features [25]. For example, when the number of the features in a turned part increased from 13 to 16, the computation time of a deterministic algorithm sharply increased from 29.95 s to 1464.7 s [25]. Comparatively, the computation time of a meta-heuristic increased from 0.81 s to only 1.66 s [26]. Meta-heuristics have become increasingly popular because they require much shorter computation time than that of deterministic algorithms for the large problems [26]. However, meta-heuristics do not guaranty finding the optimal solution and can get trapped by local optima. Hence, there is a need to select a suitable meta-heuristic for a given problem. Hu et al. [16] verified that Ant Colony Optimisation (ACO) can effectively solve the time-aware feature sequencing problem. In this article, the performance of ACO on solving our specific energy-aware feature sequence problem is compared and validated in terms of the optimality of the solutions and computation time.

According to the literature from industry and academia as reviewed above, the modelling for the NCE, in particular the SCE, is still not sufficient. Moreover, the optimisation approach for reducing the NCE through adjusting the PFS in a single machine environment has also not been well explored yet. These important gaps motivated the research presented in this paper. The developed model for the SCE and the corresponding optimisation approach based on ACO are introduced in following sections.

3. Problem statement and modelling

Considering a part, all of its n features can be denoted as a finite set $F_C = \{F_i\}_{i=1}^{n}$. When machining the part, the value of the NCE is also affected by the start and end positions of the tool. Thus, they are defined as two virtual features for the part, denoted by F_0 and F_{n+1}, respectively. In this research background, there is a finite set of $n+2$ features $F = \{F_i\}_{i=0}^{n+1}$ for an n-feature part. The F_C is a subset of the $F(F_C \subset F)$.

In Fig. 1, a part with two features (F_1 and F_2) is used as an illustrative example to show that the different PFSs can result in different values of NCE. The spindle rotation speeds for processing F_1 and F_2 are 500 rpm and 800 rpm, respectively. The start and end positions of the tool, which are virtual features, are denoted as F_0 and F_3, respectively. Two PFSs can be adopted: F_0-F_1-F_2-F_3 and F_0-F_2-F_1-F_3. The tool paths of these two PFSs are labelled by blue solid lines and red dashed lines, respectively, in Fig. 1. The spindle acceleration and deceleration during machining are marked as "↻" and "↺", respectively. The corresponding power profiles of the machine tool when processing the aforementioned two PFSs are shown in Fig. 2. The power profiles are developed based on the measured data and the prediction method by Jia [10] and Dahmus and Gutowski [27].

In Fig. 2, the areas filled with blue or red nets represent TPE. The areas filled with forward slashes and back slashes represent ASE and DSE, respectively, and the blank areas represent CE. Normally, tool changes are required during machining which results in TCE, although it is not the case in this example. This research focuses on the effect of the PFSs on the NCE which is the sum of all the TPE, TCE, and SCE. The NCE between finishing cutting the feature F_p and the beginning of cutting its post-feature F_q on the sequence can be expressed as:

$$E_{non}^{(F_p,F_q)} = E_{tp}^{(F_p,F_q)} + E_{tc}^{(F_p,F_q)} + E_{src}^{(F_p,F_q)} \tag{1}$$

where $E_{non}^{(F_p,F_q)}$, $E_{tp}^{(F_p,F_q)}$, $E_{tc}^{(F_p,F_q)}$, and $E_{src}^{(F_p,F_q)}$ ($0 \le p \le n$, $1 \le q \le n+1$, and $p \ne q$) represent the NCE, TPE, TCE, and SCE, respectively, from the feature F_p to its post-feature F_q. The detailed models for $E_{tp}^{(F_p,F_q)}$ and $E_{tc}^{(F_p,F_q)}$ can be found in Hu et al. [14]. By executing the non-cutting operations from F_p to F_q, there can be more than one change for the spindle rotation speed. Thus, a finite set of energy consumption for m changes of spindle rotation speed $C = \{C_j^{(F_p,F_q)}\}_{j=1}^{m}$ is employed to indicate the SCE between two features. $E_{src}^{(F_p,F_q)}$ can be expressed as the following:

$$E_{src}^{(F_p,F_q)} = \sum_{j=1}^{m} C_j^{(F_p,F_q)} \tag{2}$$

where $C_j^{(F_p,F_q)}$ is the energy consumption for the j-th change of the spindle rotation speed during the non-cutting operations from F_p to F_q. The effect of the different PFSs on the value of the NCE and the SCE can be seen by comparing the filled areas in Fig. 2(a) and (b). The goal of this research is to determine the optimal PFS for a part that minimises the total NCE. All of the positions of the features in a sequence can be denoted as a finite set $S = \{S_l\}_{l=1}^{n+2}$, because as the aforementioned definition, there are $n+2$ features for an n features part. S_l indicates the feature at the l-th position of a sequence. For example, $S_l = F_p$ indicates the feature at the l-th position of a sequence is F_p. For any part, the feature at the 1-st position and the $n+2$-th position is F_0 ($S_1 = F_0$) and F_{n+1} ($S_{n+2} = F_{n+1}$), respectively. Then, the objective function for minimising the NCE based on a specific PFS can be expressed as:

$$minimise\ E_N = \sum_{l=1}^{n+1} E_{non}^{(S_l,S_{l+1})} \tag{3}$$

where E_N is the total NCE based on a specific PFS and $E_{non}^{(S_l,S_{l+1})}$ is the NCE between the feature at the l-th position and the feature at the $l+1$-th position of a sequence. Its value can be obtained according to Expression (1). Constraints of the model are developed according to the precedence constraints among the features [25]. A feasible PFS must satisfy all constraints. The total NCE for the corresponding PFS is set to infinity "∞" once any feature and its pre- or post-features in a sequence violate any constraint.

Then, in Expression (2), the $C_j^{(F_p,F_q)}$ can be expressed as [28]:

$$C_j^{(F_p,F_q)} = \int_0^{t_{Cj}^{pq}} P_{Cj}^{pq}\, dt \tag{4}$$

where P_{Cj}^{pq} is the power of a machine tool during the j-th speed change of the spindle rotation in the non-cutting operations from F_p to F_q. The power of a machine tool during the speed change of the spindle rotation can be divided to two parts: the basic power of the machine tool and the power of the spindle system [27] as shown in Fig. 2. Thus, P_{Cj}^{pq} is expressed as:

$$P_{Cj}^{pq} = P_0 + P_{cj}^{pq} \tag{5}$$

where P_0 is the basic power of the machine tool and P_{cj}^{pq} is the

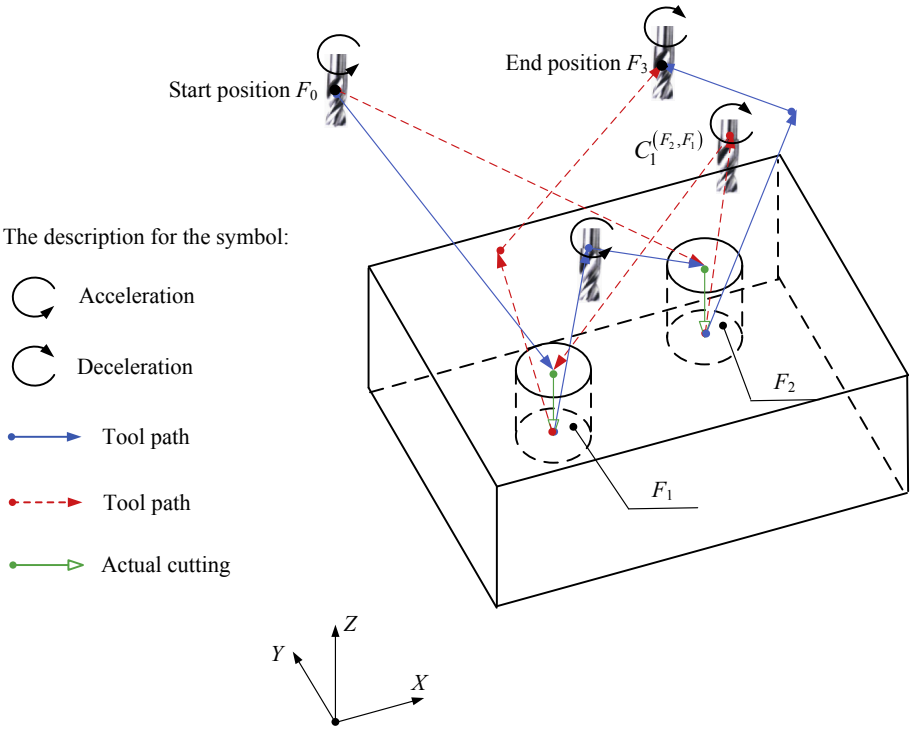

Fig. 1. A two-feature part with two feasible PFSs.

power of the spindle system during the j-th speed change of the spindle rotation in the non-cutting operations from F_p to F_q.

For a spindle acceleration, the model developed by Lv [21] can be employed and modified to model the P_{cj}^{pq} as:

$$P_{cj}^{pq} = B_{SR} \times \left(n_{Sj}^{pq} + \frac{30\alpha_A t}{\pi} \right) + C_{SR} + T_s \times \left(\frac{\pi n_{Sj}^{pq}}{30} + \alpha_A t \right) \tag{6}$$

where n_{Sj}^{pq} is the initial speed of the spindle for the j-th speed change of spindle rotation, B_{SR} and C_{SR} are the monomial coefficient and constant in the model, which are obtained by linear regression based on the power data of machine tools [29], and α_A and T_s are the angular acceleration and the acceleration torque of a spindle, respectively, which are obtained by experiment measurements.

For a spindle deceleration, if there is no energy-recycling device installed on the machine tool, the power consumption during deceleration equals to the basic power of the machine tool. Thus, $P_{cj}^{pq} = 0$. Otherwise, if the energy-recycling devices have been installed, the power level during deceleration can be negative as shown in Fig. 2 because the energy is recovered by the energy-recycling devices. Based on the measured power data, there is a linear relation between the average power of the spindle system and the speed interval of deceleration. Hence, a linear equation is employed to model P_{cj}^{pq} as:

$$P_{cj}^{pq} = B_{SRD} \times \left(n_{Ej}^{pq} - n_{Sj}^{pq} \right) + C_{SRD} \tag{7}$$

where n_{Ej}^{pq} is the end speed of the spindle for the j-th speed change of the spindle rotation; B_{SRD} and C_{SRD} are the monomial coefficient and constant, which are obtained by linear regression based on the measured power data.

In Expression (4), t_{Cj}^{pq} is the time for the j-th speed change of the spindle rotation during the non-cutting operations from F_p to F_q, which is calculated by:

$$t_{Cj}^{pq} = \frac{2\pi \left(n_{Ej}^{pq} - n_{Sj}^{pq} \right)}{60\alpha_A}. \tag{8}$$

In the next section, the algorithm for finding the optimal PFS in terms of the NCE minimisation is introduced.

4. Solution algorithms

Ant Colony Optimisation (ACO) is selected to search for the optimal PFS, by using the minimisation of NCE as the objective. Besides, three other algorithms including Depth-First Search (DFS), Genetic Algorithm (GA) and Particle Swarm Optimisation (PSO) are used as the benchmarks for the comparison and verification of ACO. ACO is introduced in detail as follows.

ACO is a meta-heuristic and probabilistic optimisation technique that imitates the behaviour of ants to discover the best path between their colony and a source of food via artificial pheromone trails [30]. A flowchart of ACO is shown in Fig. 3. At the beginning, ACO parameters are set, including α, β, ρ, Q, and K to denote the relative importance of the pheromone, the relative importance of the heuristic information, the evaporation rate, the constant, and the number of ants, respectively. All of the K ants are placed in the starting feature and then each ant continues to select the next feature to be visited through a stochastic transition rule until all ants have reached the end feature. After all of the K ants have reached the end feature, the optimal paths till now are determined and the amount of pheromones on each edge between the features are updated according to a pheromone update rule. The process of all of the K ants moving from the starting feature to the end feature is regarded as an iteration. This iteration process is repeated until a stopping condition has been met. The stopping condition can be the specified maximum number of iterations reached.

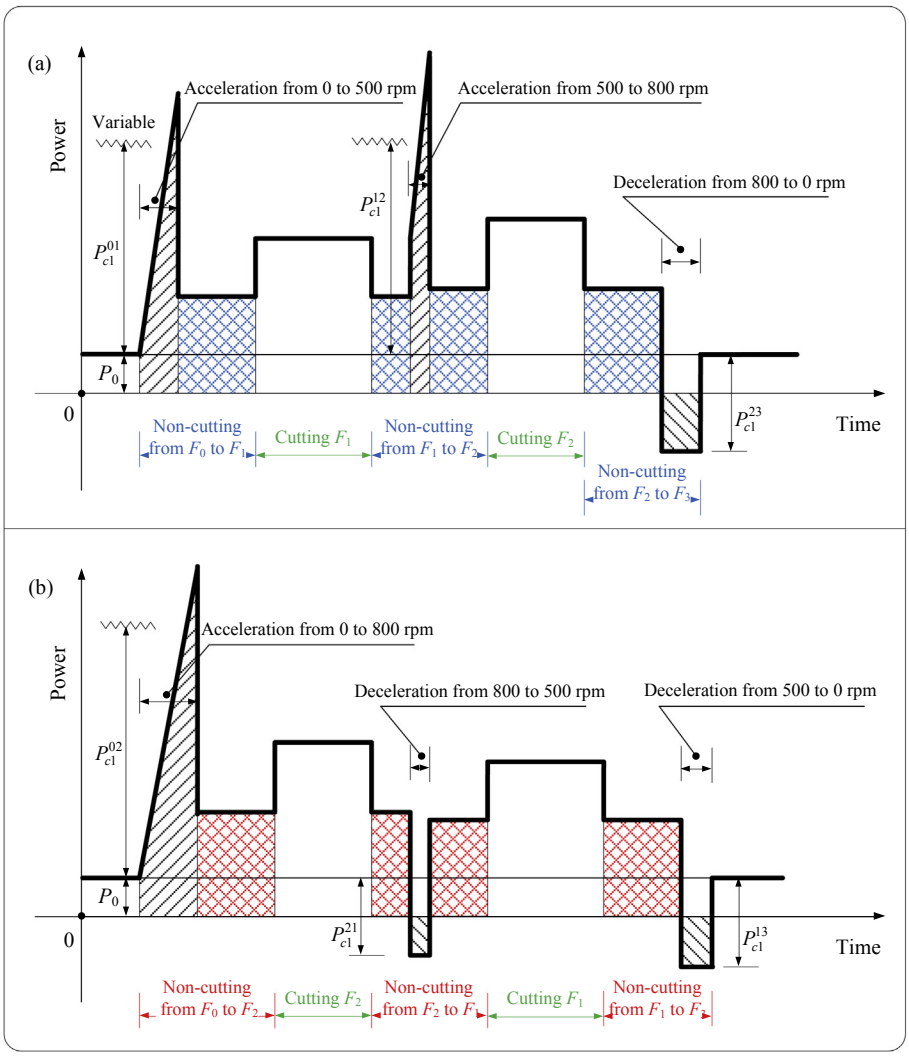

Fig. 2. Power profiles of the two PFSs: (a) F_0–F_1–F_2–F_3; (b) F_0–F_2–F_1–F_3.

4.1. The stochastic transition rule

Each ant selects the next feature to visit through a stochastic transition rule [17]. In this rule, the edge with more pheromones and heuristic information is more likely to be selected. Specifically, when the k-th ant is in the feature F_p, the probability of going to feature F_q is:

$$P_{pq}^{k} = \begin{cases} \dfrac{(\tau_{pq})^{\alpha}\cdot(\eta_{pq})^{\beta}}{\sum_{g\in N_p^k}(\tau_{pg})^{\alpha}\cdot(\eta_{pg})^{\beta}} & \text{if } q\in N_p^k, \\ 0 & \text{otherwise}, \end{cases} \tag{9}$$

where P_{pq}^{k} is the probability of going to the feature F_q for the k-th ant in the feature F_p, g is the index for a feature, N_p^k is the set of indices for the features not yet visited by the k-th ant, τ_{pq} is the amount of pheromones on the edge between F_p and F_q, which is updated according to Rule (10), η_{pq} is the heuristic information on the edge between F_p and F_q, and α and β are the parameters to control the relative importance of the pheromone and the heuristic information, respectively. η_{pq} is calculated by the reciprocal of Expression (1) as $\eta_{pq} = \frac{1}{E_{non}^{(F_p,F_q)}}$.

4.2. The pheromone update rule

At each iteration, the amount of pheromones on each edge between the features is updated according to the pheromone update rule [17], and the variables in the rule are obtained from the K paths (PFSs) constructed by the K ants in an iteration. The pheromone update rule is given by:

$$\tau_{pq} \leftarrow (1-\rho)\cdot\tau_{pq} + \sum_{k=1}^{K}\Delta\tau_{pq}^{k} \tag{10}$$

where ρ is the evaporation rate, K is the number of ants, and $\Delta\tau_{pq}^{k}$ is the amount of pheromones laid on the edge (p, q) by the k-th ant at an iteration, which is calculated by:

$$\Delta\tau_{pq}^{k} = \begin{cases} \dfrac{Q}{L_k} & \text{if the } k-\text{th ant used edge}(p,q)\text{in its path}, \\ 0 & \text{otherwises}, \end{cases} \tag{11}$$

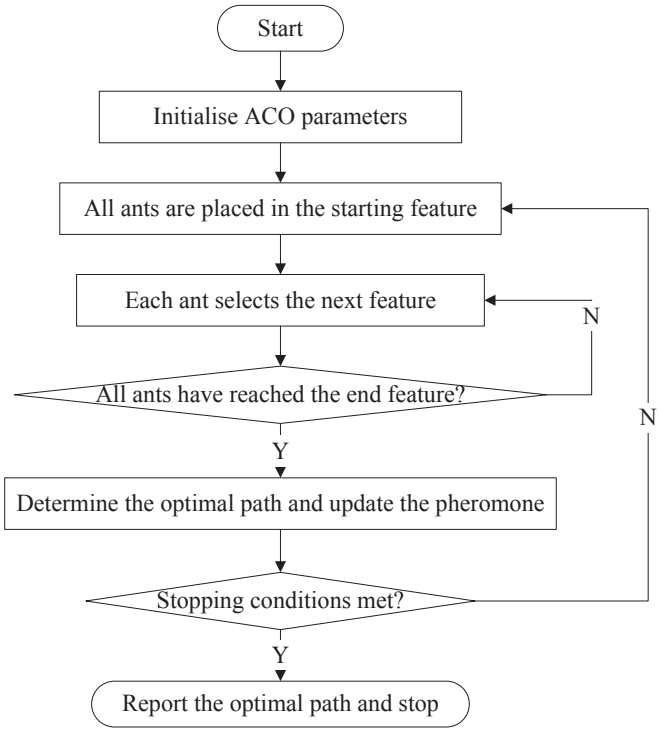

Fig. 3. A flowchart of Ant Colony Optimisation.

where Q is a constant and L_k is the energy consumption for the k-th ant's path ($L_k = E_N$).

5. Case study

5.1. Case description, modelling and optimisation

Two parts were used as the case studies to validate the developed mathematic model and the optimisation approach. Part A has 12 actual features (holes) denoted by F_1–F_{12} and 2 virtual features (F_0 and F_{13}), as shown in Fig. 4. Part B has 15 actual features denoted by F_1–F_{15} and 2 virtual features (F_0 and F_{16}), as shown in Fig. 5. For part B, the feature F_1 (plain) should be processed prior to any other features F_i ($2 \le i \le 15$). A vertical machining centre (XHF-714F) manufactured by Hangzhou CNC Machine Tool Co., Ltd. of China was used to process the two parts. The experiment set-up for the power data collection on the XHF-714F is the same as that in Hu et al. [13]. The key parameters of the XHF-714F required for the calculation of the NCE are listed in Table 1. They have been obtained through experiment measurements and regression analysis based on the method developed by Lv [21]. The process parameters defining the spindle rotation speed for each feature in part A and part B are listed in Tables 2 and 3. They have been obtained from the process files. On the basis of the above and the additional case information provided in Hu et al. [14], the NCE can be calculated.

For part A, there are 169 [(14-1)*(14-1)] possible pairs of features in its solution space. Similarly, there are 256 [(17-1)*(17-1)] possible pairs of features for part B. In the following, the value calculation procedure for the NCE between processing F_1 and F_5 ($E_{non}^{(F_1,F_5)}$) is used as an example.

Based on the above and Expression (1), the NCE from the feature F_1 to F_5 is modelled as:

$$E_{non}^{(F_1,F_5)} = E_{tp}^{(F_1,F_5)} + E_{tc}^{(F_1,F_5)} + E_{src}^{(F_1,F_5)}$$

where $E_{tp}^{(F_1,F_5)}$, $E_{tc}^{(F_1,F_5)}$, and $E_{src}^{(F_1,F_5)}$ are the TPE, TCE, and SCE from F_1 to F_5, respectively. By calculating the value of $E_{tp}^{(F_1,F_5)}$ and $E_{tc}^{(F_1,F_5)}$ based on the model in Hu et al. [14], they are 3387.98J and 0J, respectively. There is only one change of the spindle rotation speed within this case, so according to Expression (2), $E_{src}^{(F_1,F_5)}$ is: $E_{src}^{(F_1,F_5)} = C_1^{(F_1,F_5)}$.

The spindle rotation speeds for F_1 and F_5 are 500 rpm and 700 rpm according to Table 2, so $n_{S1}^{15} = 500$ rpm and $n_{E1}^{15} = 700$ rpm and the 1-st change of the spindle rotation speed from F_1 to F_5 is acceleration. Then, Equations (4) and (5) are employed to calculate $C_1^{(F_1,F_5)}$ as:

$$C_1^{(F_1,F_5)} = \int_0^{t_{Cj}^{15}} \left(P_0 + P_{c1}^{15}\right) dt$$

where P_{c1}^{15} is the power of the spindle system during the 1-st speed change of the spindle rotation in the non-cutting operations from F_1 to F_5 and t_{C1}^{15} is the corresponding time for the speed change of the spindle rotation. According to Table 1, the basic power of the XHF-714F is $P_0 = 371.0$W. According to Equation (6) and the values of B_{SR}, C_{SR}, α_A, and T_s in Table 1, P_{c1}^{15} can be calculated as:

$$\begin{aligned} P_{c1}^{15} &= 0.086 \times \left(500 + \frac{30 \times 1047.20 \times t}{\pi}\right) + 14.76 + 62.12 \\ &\quad \times \left(\frac{\pi \times 500}{30} + 1047.20 \times t\right) \\ &= 65912.066t + 3310.356 \text{ W}. \end{aligned}$$

According to Equation (8), t_{C1}^{15} can be calculated as:

$$t_{C1}^{15} = \frac{2\pi(n_{E1}^{15} - n_{S1}^{15})}{60\alpha_A} = \frac{2\pi \times (700 - 500)}{60 \times 1047.20} = 0.020\text{s}.$$

As a result, $E_{src}^{(F_1,F_5)}$ is calculated as:

$$\begin{aligned} E_{src}^{(F_1,F_5)} = C_1^{(F_1,F_5)} &= \int_0^{0.020} (371.0 + 65912.066t + 3310.356) dt \\ &= 86.81\text{J}. \end{aligned}$$

By summing the values of $E_{tp}^{(F_1,F_5)}$, $E_{tc}^{(F_1,F_5)}$, and $E_{src}^{(F_1,F_5)}$, the NCE from F_1 to F_5 is calculated as:

$$E_{non}^{(F_1,F_5)} = 3387.98 + 0 + 86.81 = 3474.8\text{J}.$$

The value of $E_{non}^{(F_1,F_5)}$ and the other 168 NCE values for part A that have been determined based on the same value calculation procedure are listed in Table 4. Moreover, the 256 NCE values for part B are directly given in Table 5.

The data in Tables 4 and 5 are the input data of the optimisation approach. Ant Colony Optimisation (ACO) is employed as our optimisation approach. ACO and all of the other algorithms are developed on a software platform Dev C++ 5.11.0 with the programming language C++. The parameters of the computation facility used for the experiments are as follows: Intel (R) Core (TM) i7-2630 QM CPU with 2.00 GHz, 4.00 GB RAM, and Windows 7 (64bit). The parameter values used for the ACO are obtained by tuning, and their values are as follows: population size= 50, $\alpha = 1.0$, $\beta = 4.0$, evaporation rate $\rho = 0.1$, $Q = 500$, and iteration= 300, as listed in Table 6. By running the developed ACO 20 times for part A and part B, the minimum NCE that ACO can

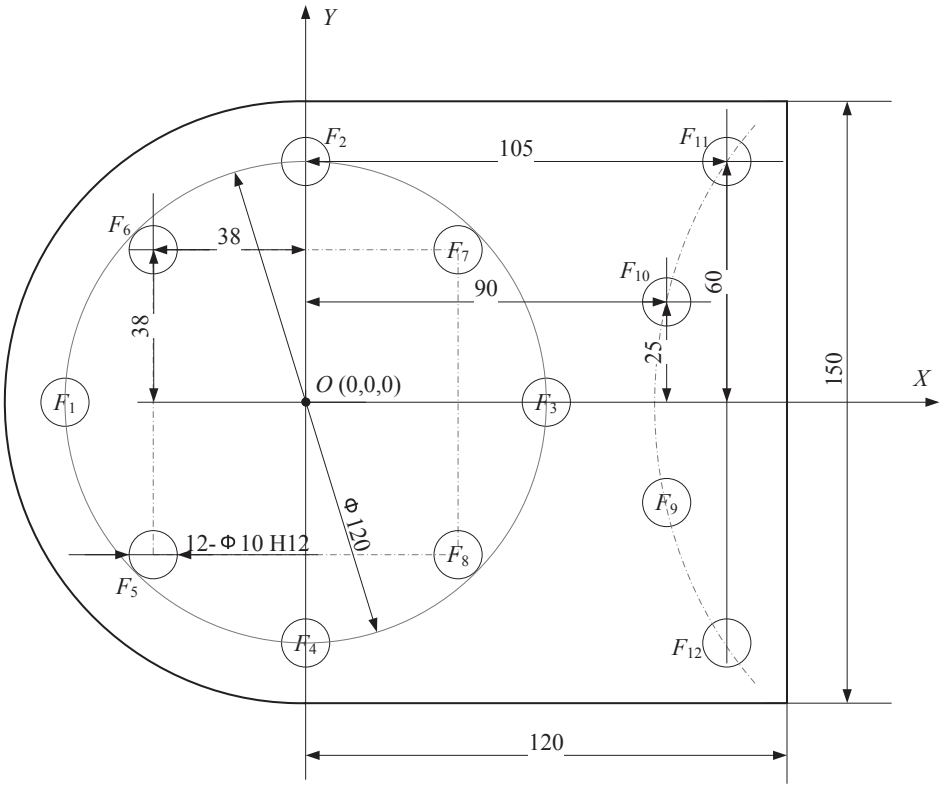

- F_0, F_{13} (-120,-105,70)

Fig. 4. Part A with 12 actual features and 2 virtual features.

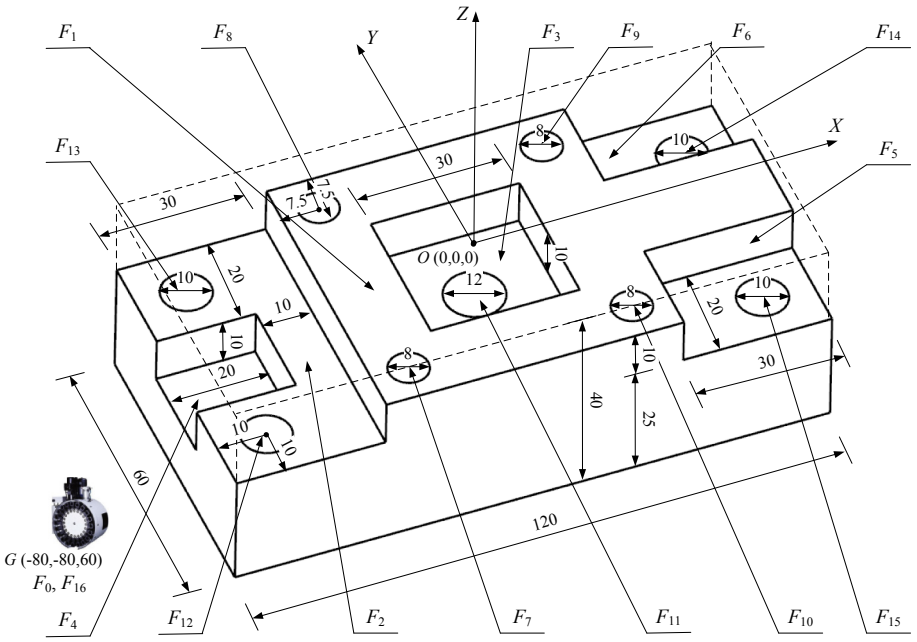

Fig. 5. Part B with 15 actual features and 2 virtual features.

achieve is 49579J and 106703J, respectively. The corresponding PFS are F_0–F_5–F_4–F_8–F_9–F_{12}–F_{11}–F_{10}–F_3–F_7–F_2–F_6–F_1–F_{13} and F_0–F_1–F_2–F_5–F_6–F_3–F_4–F_7–F_{10}–F_9–F_8–F_{12}–F_{13}–F_{14}–F_{15}–F_{11}–F_{16}, respectively. Besides, the average NCE for part A and part B is 49815J and 106703J, and the average computation time is 0.57s and 0.68s. The results are summarised in Table 7.

5.2. Results analysis and discussion

In this section, the potentiality and effectiveness of the proposed

Table 1
Parameters of the machining centre (XHF-714F) in the power models.

Item	Parameter
Basic power of the machine tool [W] P_0	371.0
Monomial coefficient and constant in the spindle rotation power model (B_{SR}, C_{SR})	(0.086, 14.76)
Monomial coefficient and constant in the spindle deceleration power model (B_{SRD}, C_{SRD})	(1.704, −52.77)
Angular acceleration of the spindle [rad/s^2] α_A	1047.20/-923.998
Acceleration torque of the spindle [N·m] T_s	62.12

Table 2
Spindle rotation speed for each feature in part A.

The i-th feature	Spindle rotation speed [rpm]	The i-th feature	Spindle rotation speed [rpm]
F_0, F_{13}	0	F_7, F_8	650
F_1, F_3	500	F_9, F_{10}	450
F_2, F_4	550	F_{11}, F_{12}	750
F_5, F_6	700		

Table 3
Spindle rotation speed for each feature in part B.

The i-th feature	Spindle rotation speed [rpm]
F_0, F_{16}	0
F_1	2600
F_2, F_3, F_4, F_5 F_6	2200
F_7, F_8, F_9, F_{10}, F_{12}, F_{13}, F_{14}, F_{15}	600
F_{11}	500

approach in reducing the NCE is analysed and demonstrated. Besides, the performance of ACO for this specific optimisation problem is discussed and validated based on the comparison with other algorithms.

5.2.1. Energy savings benefit from our approach

To demonstrate the effectiveness of the developed approach in reducing the NCE, the following comparison is conducted. A PFS produced by the Bottom-to-Top (BTT) [31] serves as the benchmark to represent the traditional sequencing technique to arranging the PFS without the energy-saving consideration. The benchmark PFSs of part A and part B are F_0–F_4–F_{12}–F_8–F_5–F_9–F_3–F_1–F_{10}–F_6–F_7–F_2–F_{11}–F_{13} and F_0–F_1–F_2–F_5–F_{12}–F_{15}–F_{10}–F_7–F_3–F_4–F_{11}–F_6–F_{14}–F_{13}–F_8–F_9–F_{16}, respectively. The NCE for the benchmark PFSs of part A and part B are 54300J and 153362J, respectively. In comparison, the minimum NCE for the PFSs of part A and part B based on our approach are 49579J and 106703J, respectively. Thus, 8.70% [(54300-49579)/54300] and 30.42% [(153362-106703)/153362] of the NCE for part A and part B can be saved. More percentage of the NCE for part B is saved than that of part A, partly because the difference between the spindle rotation speeds of the features in part B is larger than that of part A.

In addition, by using the sequencing approach developed by Hu et al. [13], the PFS of part B obtained is F_0–F_1–F_2–F_{11}–F_{15}–F_{14}–F_{13}–F_{12}–F_8–F_9–F_{10}–F_7–F_5–F_6–F_3–F_4–F_{16} and the NCE for this PFS is 108445J. Thus, compared with the approach developed by Hu et al. [13], our approach can save 1.61% [(108445-106703)/108445] more of the NCE for part B.

5.2.2. Verification of the performance of ACO

To verify the performance of ACO, a deterministic algorithm, Depth-First Search (DFS), is employed because it can always accurately find the global optimal solution [32]. Based on DFS, the global minimum NCE for part A and B are 49537J and 106703J, respectively. The corresponding PFS for part A is F_0–F_1–F_6–F_2–F_7–F_{10}–F_{11}–F_{12}–F_9–F_3–F_8–F_4–F_5–F_{13} and the corresponding PFS for part B is the same as that produced by ACO. Based on the comparison with the results obtained using DFS, ACO only achieves the near-minimum NCE of 49579J for part A in 20 trials, and it is remarkable that ACO achieves the global minimum NCE of 106703J in each trial (20 times) for part B, as summarised in Table 7. Interestingly, the solutions of part B obtained using ACO are much better than that of part A, although the design of part B is more complex than that of part A. There is probably a relationship between the design of the parts and the performance of ACO in solution quality.

In average, the solutions obtained using ACO are only 0.562% [(49815-49537)/49537] and 0% [(106703-106703)/106703] inferior than the global optimum for part A and part B. Thus, the performance of ACO is excellent in solution quality for this specific

Table 4
Non-cutting energy consumption between the features in part A.

Energy [J]	F_1	F_2	F_3	F_4	F_5	F_6	F_7	F_8	F_9	F_{10}	F_{11}	F_{12}	F_{13}
F_0	5086.5	5318.8	5760.7	4918.4	4100.5	4428.4	4957.3	4765.4	6268.2	6394.5	5137.9	4835.0	∞
F_1	∞	4373.9	4915.9	4373.9	3474.8	3474.8	4102.3	4102.3	5573.0	5573.0	4268.9	4268.9	1089.8
F_2	4685.1	∞	4685.1	4381.1	3806.7	3484.9	3658.6	3980.4	5341.9	5215.7	3715.5	4051.0	1622.4
F_3	4915.9	4373.9	∞	4373.9	3928.6	3928.6	3648.4	3648.4	4802.3	4802.3	3530.3	3530.3	1764.1
F_4	4685.1	4381.1	4685.1	∞	3484.9	3806.7	3980.4	3658.6	5215.7	5341.9	4051.0	3715.5	1222.0
F_5	4421.4	4449.4	4880.4	4123.7	∞	3479.7	4004.1	3812.2	5410.0	5536.3	4150.9	3959.1	1008.6
F_6	4421.4	4123.7	4880.4	4449.4	3479.7	∞	3812.2	4004.1	5536.3	5410.0	3959.1	4150.9	1336.5
F_7	4879.4	4123.0	4421.7	4447.4	3827.0	3635.1	∞	3675.4	5066.8	4916.3	3486.7	3747.0	1702.5
F_8	4879.4	4447.4	4421.7	4123.0	3635.1	3827.0	3675.4	∞	4916.3	5066.8	3747.0	3486.7	1510.6
F_9	5185.5	4644.9	4417.4	4518.6	4072.5	4198.8	3909.3	3759.7	∞	4777.0	3533.9	3301.5	1896.0
F_{10}	5185.5	4518.6	4417.4	4644.9	4198.8	4072.5	3759.7	3909.3	4777.0	∞	3301.5	3533.9	2022.3
F_{11}	5373.5	4505.5	4623.6	4842.2	4301.5	4109.6	3811.5	4073.1	5011.2	4772.4	∞	3520.5	2179.9
F_{12}	5373.5	4842.2	4623.6	4505.5	4109.6	4301.5	4073.1	3811.5	4772.4	5011.2	3520.5	∞	1877.0

Table 5
Non-cutting energy consumption between the features in part B.

Energy [J]	F_1	F_2	F_3	F_4	F_5	F_6	F_7	F_8	F_9	F_{10}	F_{11}	F_{12}	F_{13}	F_{14}	F_{15}	F_{16}
F_0	3103.3	2532.3	11460.0	10634.1	11266.1	11507.8	15097.5	15304.0	15496.6	15383.0	17213.0	15511.5	15700.0	16193.5	16092.5	∞
F_1	∞	1566.1	12070.9	11245.1	11877.1	12118.7	15708.4	15915.0	16107.5	15993.9	17824.0	16122.5	16310.9	16804.4	16703.4	611.0
F_2	2182.7	∞	12628.9	11803.1	12435.1	12676.7	16266.4	16473.0	16665.5	16551.9	18382.0	16680.5	16868.9	17362.4	17261.5	1169.0
F_3	11504.6	10933.5	∞	1090.1	1007.6	967.2	14732.1	14938.7	15131.2	15017.6	17119.7	15365.3	15553.7	16047.2	15946.3	379.2
F_4	11965.4	11394.3	2392.8	∞	2440.6	2425.4	15192.9	15399.5	15592.0	15478.4	17580.5	15826.1	16014.5	16508.0	16407.1	840.0
F_5	12698.6	12127.6	2354.1	2370.0	∞	1667.1	15926.2	16132.7	16325.3	16211.7	18313.8	16559.3	16747.8	17241.3	17140.3	1573.2
F_6	12784.5	12213.4	2354.1	2370.0	1667.1	∞	16012.0	16218.6	16411.1	16297.5	18399.6	16645.2	16833.6	17327.1	17226.2	1659.1
F_7	12706.7	12135.6	12296.7	11470.9	12102.9	12344.5	∞	5871.1	6063.7	5950.1	17051.9	15078.3	15266.8	15760.3	15659.3	836.7
F_8	12913.2	12342.1	12503.2	11677.4	12309.4	12551.0	5871.1	∞	5950.1	6063.7	17258.4	15284.9	15473.3	15966.8	15865.8	1043.3
F_9	13105.8	12534.7	12695.8	11870.0	12502.0	12743.6	6063.7	5950.1	∞	5871.1	17451.0	15477.4	15665.9	16159.4	16058.4	1235.8
F_{10}	12992.2	12421.1	12582.2	11756.4	12388.4	12630.0	5950.1	6063.7	5871.1	∞	17337.4	15363.8	15552.3	16045.8	15944.8	1122.2
F_{11}	14012.2	13441.1	13874.2	13048.4	13680.4	13922.0	16241.8	16448.4	16640.9	16527.3	∞	15386.0	15574.4	16067.9	15966.9	1144.4
F_{12}	13199.6	12628.6	13008.8	12183.0	12815.0	12813.7	15157.3	15363.8	15556.4	15442.8	16274.9	∞	5926.5	6485.6	6384.7	804.3
F_{13}	13388.1	12817.0	13197.3	12371.4	13003.4	13245.1	15345.7	15552.3	15744.8	15631.2	16463.4	5926.5	∞	6384.7	6485.6	992.8
F_{14}	13881.6	13310.5	13690.8	12864.9	13496.9	13738.6	15839.2	16045.8	16238.3	16124.7	16956.9	6485.6	6384.7	∞	5926.5	1486.3
F_{15}	13780.6	13209.6	13589.8	12763.9	13395.9	13637.6	15738.2	15944.8	16137.3	16023.7	16855.9	6384.7	6485.6	5926.5	∞	1385.3

optimisation problem. According to Table 7, the computation time of ACO for part A and part B is 99.10% [(63.57−0.57)/63.57] and 98.15% [(36.84−0.68)/36.84] less than that of DFS, which validates the superiority of ACO in computation time.

5.2.3. Comparison of ACO with other meta-heuristics

The performance of ACO is compared with other meta-heuristics, such as the standard Genetic Algorithm (GA) and Particle Swarm Optimisation (PSO). It has already been verified by a previous study [13] that GA can effectively solve the energy-aware feature sequencing problem when MTE is regarded as the optimisation objective, thus GA is compared with ACO for solving the new single objective optimisation problem. Besides, PSO is selected and compared with ACO for its good performance in solving the time-aware feature sequencing problem [33]. The parameter values used for GA and PSO have been obtained by tuning and are listed in Table 6. Each algorithm runs 20 times for both part A and part B. The optimisation results using the three different meta-heuristics are summarised and compared in Table 7.

According to Table 7, ACO and GA consistently outperform PSO in all of the experiments for the two parts. Although GA performs better than ACO in solution quality for part A, its computation time is longer than that of ACO. For part B, ACO outperforms GA in both solution quality and computation time. Comparatively, ACO performs best among the three standard meta-heuristics. It should be noted that the meta-heuristics are compared under the condition of our specific algorithm parameters and experiments. Although some algorithm parameters have been tuned, the optimality of these parameters is not guaranteed in this article. GA and PSO may outperform ACO through modifying the algorithm parameters, such as the crossover and mutation operators, the particle update rules, and the corresponding values of probabilities [34], but these modifications are out of the scope of this article. Besides, some novel and advanced meta-heuristics, such as Hybrid Genetic Algorithm-Ant Colony Optimisation [35], Ant Lion Optimisation Algorithm [36], and Bird-Mating Optimisation [37], have not been employed and compared in this article. In the future, research work on exploring a better algorithm for solving our problem can be conducted.

6. Conclusions and future work

It has been confirmed that the machining energy consumption of the machine tool can be reduced by adjusting the processing sequence of the features of a part (PFS) at the process planning stage [13]. However, the NCE portion has not been well explored in the previous research. In particular, the effect of the PFS on the SCE has not been understood, and the SCE normally accounts for nearly 14% of the total NCE. Thus, this research develops a novel SCE model and integrates it with the existing TPE and TCE models [14] to obtain the completed NCE model. Based on this NCE model, a new single objective optimisation problem that minimises the NCE is introduced. Then, Ant Colony Optimisation (ACO) is employed and modified as the optimisation approach to search for the optimal PFS, and the performance of ACO is compared and validated. In summary, it is the main innovation of this paper to reduce the NCE with the SCE included through feature sequencing, and the proposed model and optimisation approach for the new problem are the main contributions.

In the case study, the optimal and near-optimal PFSs for two parts with 12 and 15 features have been found. Consequently, 8.70% and 30.42% of the NCE for part A and part B are reduced, which validates the effectiveness of the developed approach. Although the solutions obtained using ACO are 0.562% and 0% inferior than the global optimum for part A and part B, the computation time of ACO

Table 6
Parameter values used in meta-heuristics: ACO, GA, and PSO.

Algorithms	Population size	Iteration	Other parameters
ACO	50	300	$\alpha = 1.0$; $\beta = 4.0$; evaporation rate $\rho = 0.1$; $Q = 500$
GA	100	300	crossover probability = 0.9; mutation probability = 0.05
PSO	50	300	inertia weight = 0.7

Table 7
Comparisons of ACO with BTT, DFS, GA, and PSO.

	Algorithms	ACO	BTT	DFS	GA	PSO
Part A	Minimum NCE achieved [J]	49579	54300	49537	49537	50215
	Times of getting minimum	0	0	20	2	0
	Average NCE of 20 trials [J]	49815	54300	49537	49685	50457
	Standard deviation of NCE	96	0.00	0.00	118	109
	Average computation time [s]	0.57	–	63.57	1.76	1.46
Part B	Minimum NCE achieved [J]	106703	153362	106703	106703	107447
	Times of getting minimum	20	0	20	2	0
	Average NCE of 20 trials [J]	106703	153362	106703	108026	107495
	Standard deviation of NCE	0.00	0.00	0.00	852	54
	Average computation time [s]	0.68	–	36.84	2.43	1.67

is at least 98.15% less than that of a deterministic algorithm. It shows the superiority of ACO in computation time. Further, ACO performs better than other meta-heuristics including GA and PSO based on the experiment results.

In this presented research, it is laborious to calculate $(n+1)^2$ NCE values one by one for a part with n actual features. Thus, the automation for the corresponding calculation can be improved. One limitation is that some other non-cutting operations, such as setup change, have not been considered. Usually, machine tools consume energy during the execution of these operations. Thus, for the next step, the energy consumption model for these operations will be developed. The single objective is another limitation. In real manufacturing circumstances, it is unrealistic to only reduce the NCE without controlling the processing time, quality, and cost. Thus, other optimisation objectives, including time, quality, and cost, should also be considered when optimising the NCE. In the future, the relationship between the design of the parts and the performance of ACO in solution quality will be explored. Besides that, research work on exploring a better algorithm for solving our problem will be conducted. Finally, the proposed energy-aware feature sequencing approach will be combined with the product design software to assist in industrial applications.

Acknowledgments

The authors would like to thank the support from the National Natural Science Foundation of China (No. U1501248), the China Scholarship Council (No. 201406320033), the EPSRC Centre for Innovative Manufacturing in Industrial Sustainability (No. EP/I033351/1), and the EPSRC Centre for Innovative Manufacturing in Intelligent Automation (No. EP/I033467/1).

Appendix A. Abbreviations and notations

The abbreviations and notations used in the problem statement, the algorithm description and throughout the paper are as follows:

Abbreviations

ACO	ant colony optimisation
ASE	energy consumption of a machine tool for the acceleration of the spindle rotation
CE	cutting energy consumption of a machine tool
BTT	bottom-to-top
DFS	depth-first search
DSE	energy consumption of a machine tool for the deceleration of the spindle rotation
GA	genetic algorithm
MTE	machining energy consumption of a machine tool
NCE	non-cutting energy consumption of a machine tool
PFS	processing sequence of the features of a part
PFSs	processing sequences of the features of a part
PSO	particle swarm optimisation
rpm	revolutions per minute
SCE	energy consumption of a machine tool during the change of spindle rotation speed
TCE	energy consumption of a machine tool during tool change
TPE	energy consumption of a machine tool during tool path

Nomenclature

Feature sequencing problem

n	number of features in a part
i	index for a feature in a part
F_C	a finite set of n features for a part, $F_C = \{F_i\}_{i=1}^{n}$
F_0	a virtual feature for a specific part to denote the start position of the tool
F_{n+1}	a virtual feature for a specific part to denote the end position of the tool
F	a finite set of $n+2$ features for a part in the machining environment, $F = \{F_i\}_{i=0}^{n+1}$, $F_C \subset F$
j	index for a change of the spindle rotation speed during the non-cutting operations from a feature to its post-feature
m	number of changes for the spindle rotation speed during the non-cutting operations from a feature to its post-feature
S	a finite set of $n+2$ positions of features in a sequence, $S = \{S_l\}_{l=1}^{n+2}$
S_l	l-th position of a sequence
l	index for a position in a sequence

Energy consumption

$E_{non}^{(F_p,F_q)}$ NCE from the feature F_p to its post-feature F_q [J]
$E_{tp}^{(F_p,F_q)}$ TPE from the feature F_p to its post-feature F_q [J]
$E_{tc}^{(F_p,F_q)}$ TCE from the feature F_p to its post-feature F_q [J]
$E_{src}^{(F_p,F_q)}$ SCE from the feature F_p to its post-feature F_q [J]
C a finite set of energy consumption for m changes of spindle rotation speed $C = \{C_j^{(F_p,F_q)}\}_{j=1}^{m}$ during the non-cutting operations from F_p to F_q, $(0 \le p \le n, 1 \le q \le n+1$, and $p \ne q)$
$C_j^{(F_p,F_q)}$ energy consumption for the j-th change of the spindle rotation speed during the non-cutting operations from F_p to F_q [J]
E_N total NCE based on a specific feature sequence [J]
$E_{non}^{(S_l,S_{l+1})}$ NCE between a feature at the l-th position and a feature at the $l+1$-th position of a sequence [J]
P_{Cj}^{pq} power of a machine tool during the j-th speed change of the spindle rotation in the non-cutting operations from F_p to F_q [W]
P_0 basic power of a machine tool [W]
P_{cj}^{pq} power of the spindle system during the j-th speed change of the spindle rotation in the non-cutting operations from F_p to F_q [W]
n_{Sj}^{pq} initial speed of the spindle for the j-th speed change of the spindle rotation during the non-cutting operations from F_p to F_q [rpm]
B_{SR} monomial coefficient in the spindle rotation power model
C_{SR} constant in the spindle rotation power model
α_A angular acceleration of a spindle [rad/s^2]
T_s acceleration torque of a spindle [N·m]
t_{Cj}^{pq} time for the j-th speed change of the spindle rotation in the non-cutting operations from F_p to F_q [s]
n_{Ej}^{pq} end speed of the spindle for the j-th speed change of the spindle rotation during the non-cutting operations from F_p to F_q [rpm]
B_{SRD} monomial coefficient in the spindle deceleration power model
C_{SRD} constant in the spindle deceleration power model

Ant colony optimisation

α relative importance of the pheromone
β relative importance of the heuristic information
ρ evaporation rate
Q constant of the pheromone update rule
K number of ants
k index for an ant
P_{pq}^k probability of going to the feature F_q for the k-th ant in the feature F_p
N_p^k a set of indices for the features not yet visited by the k-th ant
τ_{pq} amount of pheromones on the edge between F_p and F_q
η_{pq} heuristic information on the edge between F_p and F_q
$\Delta\tau_{pq}^k$ amount of pheromones laid on the edge (p, q) by the k-th ant at an iteration
L_k energy consumption for the k-th ant's path

Appendix B. Supplementary data

Supplementary data related to this article can be found at https://www.researchgate.net/publication/319059278_Sequencing_the_features_to_minimise_the_non-cutting_energy_consumption_in_machining_considering_the_change_of_spindle_rotation_speed.

References

[1] International Energy Agency (IEA). Tracking industrial energy efficiency and CO2 emissions. 2007. Retrieved from: https://www.iea.org/publications/freepublications/publication/tracking_emissions.pdf. Last visited: 17/6/2016.
[2] Zhou L, Li J, Li F, Meng Q, Li J, Xu X. Energy consumption model and energy efficiency of ma-chine tools: a comprehensive literature review. J Clean Prod 2016;112:3721–34.
[3] Schudeleit T, Züst S, Wegener K. Methods for evaluation of energy efficiency of machine tools. Energy 2015;93:1964–70.
[4] Cai W, Liu F, Zhou X, Xie J. Fine energy consumption allowance of workpieces in the mechanical manufacturing industry. Energy 2016;114:623–33.
[5] HEIDENHAIN. Aspects of energy efficiency in machine tools. 2011. Retrieved from: http://www.heidenhain.us/enews/stories_1011/MTmain.php. Last visited: 21/5/2016.
[6] Hong CM, Ou TC, Lu KH. Development of intelligent MPPT (maximum power point tracking) control for a grid-connected hybrid power generation system. Energy 2013;50:270–9.
[7] Ou TC. A novel unsymmetrical faults analysis for microgrid distribution systems. Int J Elec Power 2012;43(1):1017–24.
[8] Hu L, Peng T, Peng C, Tang R. Energy consumption monitoring for the order fulfilment in a ubiquitous manufacturing environment. Int J Adv Manuf Tech 2017;89(9–12):3087–100.
[9] Cai W, Liu F, Zhang H, Liu P, Tuo J. Development of dynamic energy benchmark for mass production in machining systems for energy management and energy-efficiency improvement. Appl Energ 2017;202:715–25.
[10] Jia S. Research on energy demand modeling and intelligent computing of machining process for low carbon manufacturing [dissertation]. Zhejiang University; 2014 [in Chinese].
[11] Sheng P, Srinivasan M, Kobayashi S. Multi-objective process planning in environmentally conscious manufacturing: a feature-based approach. CIRP Ann-Manuf Technol 1995;44(1):433–7.
[12] Yin R, Cao H, Li H, Sutherland JW. A process planning method for reduced carbon emissions. Int J Comput Integ M 2014;27(12):1175–86.
[13] Hu L, Peng C, Evans S, Peng T, Liu Y, Tang R, et al. Minimising the machining energy consumption of a machine tool by sequencing the features of a part. Energy 2017;121:292–305.
[14] Hu L, Liu Y, Tang R, Tiwari A. Minimising energy consumption of tool change and tool path of machining by sequencing features. 2016. http://dx.doi.org/10.13140/RG.2.2.20407.11687. Retrieved from: https://www.researchgate.net/publication/306259904_Minimising_energy_consumption_of_tool_change_and_tool_path. Last visited: 2/8/2016.
[15] Abele E, Sielaff T, Schiffler A, Rothenbücher S. Analyzing energy consumption of machine tool spindle units and identification of potential for improvements of efficiency. In: Glocalized solutions for sustainability in manufacturing; 2011. p. 280–5.
[16] Hu Q, Qiao L, Peng G. An ant colony approach to operation sequencing optimization in process planning. P I Mech Eng B-J Eng 2017;231(3):470–89.
[17] Dorigo M, Blum C. Ant colony optimization theory: a survey. Theor Comput Sci 2005;344(2):243–78.
[18] Bhaskara Reddy SV. Operation sequencing in CAPP using genetic algorithms. Int J Prod Res 1999;37(5):1063–74.
[19] Krishna AG, Rao KM. Optimisation of operations sequence in CAPP using an ant colony algorithm. Int J Adv Manuf 2006;29(1–2):159–64.
[20] Shi J, Liu F, Xu D, Chen G. Decision model and practical method of energy-saving in NC machine tool. China Mech Eng 2009;20(11):1344–6.
[21] Lv JX. Research on energy supply modeling of computer numerical control machine tools for low carbon manufacturing [dissertation]. Zhejiang University; 2014 [in Chinese].
[22] Avram OI, Xirouchakis P. Evaluating the use phase energy requirements of a machine tool system. J Clean Prod 2011;19(6):699–711.
[23] Lin CJ, Wang HP. Optimal operation planning and sequencing: minimization of tool changeovers. Int J Prod Res 1993;31(2):311–24.
[24] Gan PY, Lee KS, Zhang YF. A branch and bound algorithm based process-planning system for plastic injection mould bases. Int J Adv Manuf Tech 2001;18(9):624–32.
[25] Lee DH, Kiritsis D, Xirouchakis P. Branch and fathoming algorithms for operation sequencing in process planning. Int J Prod Res 2001;39(8):1649–69.
[26] Lee DH, Kiritsis D, Xirouchakis P. Search heuristics for operation sequencing in process planning. Int J Prod Res 2001;39(16):3771–88.
[27] Dahmus JB, Gutowski TG. An environmental analysis of machining. In: ASME 2004 international machining engineering congress and RD&D expo. 2004. p. 643–52.
[28] Xie J, Liu F, Qiu H. An integrated model for predicting the specific energy consumption of manufacturing processes. Int J Adv Manuf Technol 2016;85(5):1339–46.
[29] Lv JX, Tang RZ, Jia S, Liu Y. Experimental study on energy consumption of computer numerical control machine tools. J Clean Prod 2016;112:3864–74.

[30] Dorigo M, Gambardella LM. Ant colony system: a cooperative learning approach to the traveling salesman problem. IEEE T Evol Comput 1997;1(1):53–66.
[31] Al-Sahib NKA, Abdulrazzaq HF. Tool path optimization of drilling sequence in CNC machine using genetic algorithm. Innov Syst Des Eng 2014;5(1):15–26.
[32] Bhattacharya S, Roy R, Bhattacharya S. An exact depth-first algorithm for the pallet loading problem. Eur J Oper Res 1998;110(3):610–25.
[33] Guo YW, Mileham AR, Owen GW, Li WD. Operation sequencing optimization using a particle swarm optimization approach. P I Mech Eng B-J Eng 2006;220(12):1945–58.
[34] Ou TC, Hong CM. Dynamic operation and control of microgrid hybrid power systems. Energy 2014;66:314–23.
[35] Lin WM, Lu KH, Ou TC. Design of a novel intelligent damping controller for unified power flow controller in power system connected offshore power applications. IET Gener Transm Dis 2015;9(13):1708–17.
[36] Ali ES, Elazim SA, Abdelaziz AY. Ant lion optimization algorithm for renewable distributed generations. Energy 2016;116:445–58.
[37] Ou TC, Su WF, Liu XZ, Huang SJ, Tai TY. A modified bird-mating optimization with hill-climbing for connection decisions of transformers. Energies 2016;9(9):671.